Diffusing-Wave Spectroscopy

D. J. Pine,[1,2] D. A. Weitz,[1] P. M. Chaikin,[1,3] and E. Herbolzheimer[1]

[1]Exxon Research and Engineering, Annandale, New Jersey 08801

[2]Department of Physics, Haverford College, Haverford, Pennsylvania 19041

[3]Department of Physics, University of Pennsylvania, Philadelphia, Pennsylvania 19104

(Received 26 October 1987)

We obtain useful information from the intensity autocorrelations of light scattered from systems which exhibit strong multiple scattering. A phenomenological model, which exploits the diffusive nature of the transport of light, is shown to be in excellent agreement with experimental data for several different scattering geometries. The dependence on geometry provides an important experimental control over the time scale probed. We call this technique diffusing-wave spectroscopy, and illustrate its utility by studying diffusion in a strongly interacting colloidal glass.

Quasielastic light scattering (QELS) has found wide use in the study of many dynamic processes.[1] By monitoring of the time-dependent fluctuations in the intensity of the scattered light, it is relatively simple to extract useful information about the dynamics of the scatterers. However, this simplicity requires QELS experiments to be performed in the strictly single-scattering limit. As the concentration of scatterers increases, a multiple-scattering regime rapidly is approached, making the interpretation of the data extremely difficult. Until now, this has limited the effective application of QELS to the single-scattering regime. Very recently Maret and Wolf have reported an experimental measurement of the intensity autocorrelation function in the multiple-scattering limit and have suggested a simple way of treating the data.[2] Subsequently, Stephen derived theoretical expressions for the functional form of the autocorrelation function in the multiple-scattering limit.[3] This suggests the possibility of extending QELS to the multiple-scattering regime.

In this Letter we show that useful information about the dynamics of the scatterers can be obtained in the multiple-scattering regime by exploitation of the fact that the transport of the light is diffusive. This diffusive transport leads to autocorrelation functions which are highly dependent on the experimental geometry. However, by properly including these effects in the calculation of the autocorrelation functions, we are able quantitatively to determine their functional form. Here we show that this geometrical dependence can be exploited to probe dynamical processes on many different time scales. This both extends the application of QELS to the multiple-scattering regime and results in a new method of studying complex systems where the dynamics depend on the time scale. We call this new technique diffusing-wave spectroscopy (DWS).

We consider a system of noninteracting spherical scatterers with a diffusion coefficient D. We define a charac-teristic diffusion time $\tau_0 = 1/Dk_0^2$, where $k_0 = 2\pi/\lambda$ and λ is the wavelength of light in the medium. Then, as shown by Maret and Wolf,[2] the electric field autocorrelation function can be written as

$$G_1(\tau) \propto \int_0^\infty P(s) \exp[-(2\tau/\tau_0)(s/l^*)]\, ds, \qquad (1)$$

where τ is the delay time and $P(s)$ is the probability that the light travels a path of length s. We assume that the transport of the light is diffusive, so that the energy density, U, is described by $\partial U/\partial t = D_l \nabla^2 U$, with a diffusion coefficient $D_l \equiv cl^*/3$ and l^* the transport mean free path.[4,5] Physically, Eq. (1) reflects the fact that a diffusion path of length s corresponds to a random walk of s/l^* steps and $G_1(\tau)$ decays, on average, $\exp(-2\tau/\tau_0)$ per step. Thus $G_1(\tau)$ contains a wide distribution of decay times, with the most rapid decay times coming from the longest paths.

The key to the solution of Eq. (1) is the determination of $P(s)$ for the experimental geometry. Physically, we imagine an instantaneous pulse of light at $t=0$ which has just begun to diffuse a distance $z_0 = \gamma l^*$ inside the sample $[U_{in}(x,y,z,t) = \delta(z-z_0,t)]$, where we expect that $\gamma \approx 1$. Then $P(s)$ is proportional to the time dependence of the light intensity emerging from the sample, $P(s) \propto \hat{z} \cdot \nabla U_{out}(x,y,z,t)$. This can be determined by our solving the diffusion equation for U with the transformation $s = ct$ and subject to the condition that $U=0$ at the boundaries. In fact, by our noting that $G_1(\tau)$ is a Laplace transform of $P(s)$ the solution is simplified. Finally, for comparison with experiment, we calculate the intensity autocorrelation function, $G_2(\tau) = |G_1(\tau)|^2$. We note that while this is a physically intuitive method for obtaining $G_1(\tau)$, it can also be obtained using more sophisticated diagrammatic techniques.[3,6]

We first consider transmission through a slab of thickness L and of infinite extent. For light incident from an extended plane source and collected from a point on the
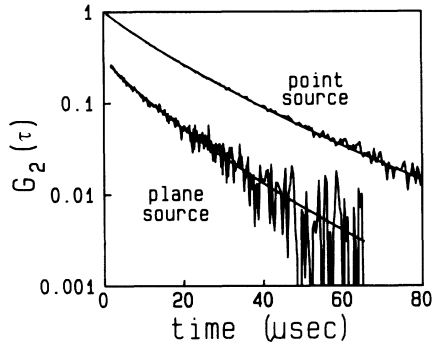
FIG. 1. Intensity autocorrelation functions vs time for transmission through 2-mm-thick cells with 0.497-μm-diam polystyrene spheres and $\phi = 0.01$. Smooth lines are fits to the data by Eqs. (2) and (3) with $l^* = 143$ μm for the point source and $l^* = 144$ μm for the plane source.

other side of the slab, we obtain

$$G_1(\tau) = \frac{L}{\gamma l^*} \frac{\sinh[\gamma(6\tau/\tau_0)^{1/2}]}{\sinh[(L/l^*)(6\tau/\tau_0)^{1/2}]}$$

$$\approx \frac{(L/l^*)(6\tau/\tau_0)^{1/2}}{\sinh[(L/l^*)(6\tau/\tau_0)^{1/2}]}, \tag{2}$$

where the second expression holds for $\tau \ll \tau_0$. By contrast, for light incident from a point source on axis with the detector, we obtain

$$G_1(\tau) \propto \int_{(6\tau/\tau_0)^{1/2}(L/l^*)}^{\infty} \frac{\zeta \sinh(\gamma l^* \zeta/L)}{\sinh \zeta} d\zeta. \tag{3}$$

The characteristic time scale is $(l^*/L)^2 \tau_0 \ll \tau_0$, reflecting the diffusive nature of the transport. We note that the experimental time scales ensure that the results are insensitive to γ. Physically, this reflects the fact that the details of the contribution of the first step are not important when the typical number of steps is $(L/l^*)^2 \gg 1$.

Typical autocorrelation functions obtained in transmission are shown in Fig. 1. We use 0.497-μm-diam polystyrene latex spheres at a volume fraction of $\phi = 0.01$ and $L = 2$ mm. Light from a 488-nm laser was focused to a point of $\simeq 50$-μm diam on one side of the sample, and the scattered light was collected from a 50-μm point on the other side with imaging optics. The resulting intensity autocorrelation function is shown in Fig. 1, curve

a. For comparison, when the incident light is expanded to a 1-cm-diam plane source, the resultant autocorrelation function is shown in Fig. 1, curve b. The data are fitted by the appropriate equations above with the assumption that $\tau_0 = 3.73$ msec, obtained from a QELS measurement at $\phi = 10^{-5}$, in the single-scattering limit. In both cases, the functional form of the autocorrelation function is well described by the appropriate formula, the only fitting parameter being l^*. We obtain $l^* = 143$ μm for the point source and $l^* = 144$ μm for the plane source. The excellent consistency confirms that the different decay rates of the autocorrelation functions in Fig. 1 are due solely to geometric effects. Physically this difference reflects the fact that for a plane source, there are more long light paths contributing to $G_2(\tau)$, resulting in a faster decay.

The first cumulant of $G_2(\tau)$ for a plane source is $\Gamma_1 = 4(L/l^*)^2/\tau_0$, as can be seen by our taking the logarithmic derivative of Eq. (2) and letting $t \rightarrow 0$. Experimentally, we find $\Gamma_1 \sim L^2$ when the sample thickness is varied from 0.3 to 3 mm. We emphasize that the control of L provides a simple and convenient method for experimentally varying the time scale probed. Finally, in contrast to conventional QELS, we find no dependence of $G_2(\tau)$ on the collection angle, as expected for multiple scattering.

The value of l^* can also be determined from static measurements of the width of the enhanced backscattering cone,[7-9] and through theoretical calculations.[8-10] Interestingly, measurements and calculations for slightly smaller spheres suggest a value of $l^* \approx 200$ μm for this volume fraction, substantially larger than the value obtained from DWS in transmission. We find similar behavior using other sphere sizes, and consistently obtain a smaller value of l^* with dynamic measurements than is obtained from static backscattering. We have ruled out absorption as the cause of this discrepancy. Equation (1) can be simply modified to include absorption and the resultant expressions account very well for data obtained from samples with absorbing dye added.[11] The origin of the differences in l^* is not known.

We can also solve the diffusion equation for a backscattering geometry, which provides additional interesting information. We consider an extended plane-wave source incident on one face of a slab of thickness L and infinite extent and calculate $G_1(\tau)$ for light collected from a point on the same face, obtaining

$$G_1(\tau) = \frac{1}{1 - \gamma l^*/L} \frac{\sinh[(L/l^*)(6\tau/\tau_0)^{1/2}(1 - \gamma l^*/L)]}{\sinh[(L/l^*)(6\tau/\tau_0)^{1/2}]} \rightarrow \exp[-\gamma(6\tau/\tau_0)^{1/2}], \quad \text{for } L \gg l^*. \tag{4}$$

In Fig. 2, we show autocorrelation functions obtained from slabs of different thicknesses containing the same sample and using an extended plane source while collecting from a point in backscattering. To ensure that all the light collected has been multiply scattered, as required by our model, we use a polarizer to select only the

polarization perpendicular to the incident light, although the behavior of the parallel polarization is nearly the same.[2] For comparison to the theoretical expressions, we plot the logarithm of $G_2(\tau)$ as a function of $(\tau/\tau_0)^{1/2}$. With use of $l^* = 143$ μm from the transmission data and
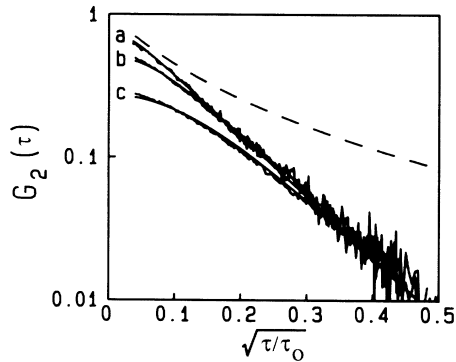
FIG. 2. Intensity autocorrelation functions vs square root of reduced time for backscattering from cells with different thicknesses L: Curve a, $L = 2.0$ mm; curve b, $L = 1.0$ mm; Curve c, $L = 0.6$ mm. The solid lines through the data are fits by Eq. (4) with l^* set equal to 143 μm and $\gamma = 2.0$. The dashed line is $G_2(\tau) \equiv |G_1(\tau)|^2$ from Eq. (5) with $\gamma = 2.0$.

FIG. 3. Intensity autocorrelation functions vs square-root time for transmission and backscattering from mixtures with 0.497-μm- ($\phi = 0.04$) and 0.312-μm-diam ($\phi = 0.01$) polystyrene spheres, with $L = 1.0$ mm. Curves a: Noninteracting mixture. Curves b: strongly interacting colloidal glass. Circles represent transmission data for the strongly interacting glass scaled by the ratio of l^* for the two samples.

for $\tau_0 = 3.73$ msec, the only unknown parameter is γ. If we compare each data set to Eq. (4), we obtain excellent agreement at all times and for all L with $\gamma = 2.0$. We obtain this same form for $G_2(\tau)$ in backscattering for all sizes of spheres that we have tried, down to diameters as small as 0.091 μm, and have found γ to vary by only $\approx 10\%$. We note in addition that the data of Maret and Wolf[2] are also well described by this form.

Since $\ln[G_2(\tau)] \sim \tau$ in Eq. (4), the slope is infinite as $\tau \to 0$ for an infinitely thick slab. In this case, there are no finite-size effects and the data would not depend on l^*. However, as can be seen in Fig. 2, the data roll over at short times. This is due to the finite thickness of the sample which cuts off the longest paths of the diffusing light which cause the decay at the shortest times,[9] and introduces an l^* dependence. It is therefore possible in principle to obtain l^* from backscattering data for finite slab thickness. The values so obtained are consistent with the dynamic transmission measurements.

We emphasize that in contrast to the case of transmission, in backscattering $G_2(\tau)$ contains contributions from paths of all lengths. Thus $G_2(\tau)$ is very sensitive to the details of how the propagating light is converted to diffusing light in the first several scattering events. We have made the simplest approximation by assuming that the conversion occurs at a single distance, γl^*, into the sample. This approach clearly agrees with the experimental data. However, the actual conversion process is considerably more complex and other approximations can lead to substantially different results.

We can modify the initial conditions of the diffusion equation to reflect the spatial dependence of this conversion. One approach is to use an exponential for U_{in}, $\exp(-z/\gamma l^*)$. This changes the form of $G_1(\tau)$ dramatically,

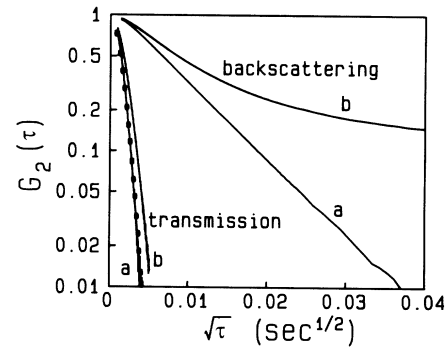$$G_1(\tau) = [1 + \gamma(6\tau/\tau_0)^{1/2}]^{-1} \quad \text{for} L \gg \gamma l^*. \tag{5}$$

Unfortunately, as shown in Fig. 2, this form fails to fit the data, particularly at longer times. We note that Stephen[3] also obtains a power-law form for the decay of $G_1(\tau)$ similar to Eq. (5) using more sophisticated diagrammatic techniques. However, his approach is exclusively for small, isotropic scatterers. By contrast, large particles scatter primarily in the forward direction, so that many scattering events are required to convert propagating light fully to diffusing energy. This suggests that the failure of an exponential form for U_{in} may arise from an inadequate accounting for this scattering anisotropy.

The problem of the conversion of propagating light to diffusing light by anisotropic scatterers is a long-standing one.[12] An alternative approach[13] is to modify the boundary conditions for the diffusion equation to account for this complex conversion. Use of these modified boundary conditions makes the expression for $G_2(\tau)$ substantially more complicated but does not change the essential form of the decay. Our expression in Eq. (4) has the advantage of simplicity while accounting for the data very well. However, a more precise description of the conversion from propagating to diffusing intensity is clearly desirable.

To illustrate the utility of DWS, we study the Brownian dynamics in dense colloidal suspensions both with and without strong Coulombic interactions. We use mixtures containing 0.312-μm-diam spheres at $\phi_a = 0.01$ and 0.497-μm-diam spheres at $\phi_b = 0.04$. In one sample, ion-exchange resin was added to decrease the electrolyte concentration; the resultant strong Coulombic repulsion caused the formation of a colloidal glass.[14] In Fig. 3, curves a, we show the measured $G_2(\tau)$ for both the transmission and backscattering geometries for the mixture containing the noninteracting (no added ion-

exchange resin) colloidal suspension. We have again used a logarithmic scale for $G_2(\tau)$ plotted as a function of τ. On this plot, $G_2(\tau)$ for backscattering is linear despite the fact that the sample is a mixture of two different sized spheres, each with its own distinct τ_0. This demonstrates that DWS is not as sensitive to polydispersity as QELS because of the additional averaging that arises in the multiple-scattering geometry.

For comparison, in Fig. 3, curves b, we show $G_2(\tau)$ measured, in both geometries, for the strongly interacting colloidal glass. In contrast to the noninteracting sample, $G_2(\tau)$ for backscattering is highly curved. This reflects the fact that in a glass, the mean square displacement of each particle is nonlinear in time. Physically, $G_2(\tau)$ contains contributions from many path lengths of the diffusing light [Eq. (1)]. The dephasing of light traversing long paths is caused by the cumulative effect of small displacements of each particle. These occur on a short time scale. By contrast, the dephasing of light traversing shorter paths requires large displacements of each particle. These are hindered in the strongly interacting glass. Experimentally, we find that the long-time behavior of $G_2(\tau)$ has a decay time of greater than 10 sec, confirming our expectation that large particle displacements are frozen.

The $G_2(\tau)$ measured in transmission contains contributions only from longer paths and thus decays much more rapidly, as seen in Fig. 3. We expect that the time for the small motions (much less than the interparticle spacing) that contribute to the dephasing is nearly identical for both samples. However, to extract τ_0 from the transmission data requires knowledge of l^*. This can be done experimentally through comparison to a sample with known τ_0, for which l^* is obtained from $G_2(\tau)$ in transmission. Then we obtain l^* for the samples of interest by exploiting the fact that the static transmission for diffusive transport scales as $l^*/(L+4l^*/3)$, provided absorption is negligible.[12] We find $l^* = 51$ μm for the noninteracting sample and 57 μm for the interacting sample, the difference reflecting the effect of the static structure factors.[10] If the time axis of the interacting sample is scaled by the ratio of these l^*, the two transmission $G_2(\tau)$ are nearly identical. The results are shown in Fig. 3; they confirm the scaling of $G_2(\tau)$ with l^*, the linear dependence of the static transmission of l^*, and that the short-time motion of the particles is essentially insensitive to the interactions.

The results presented in this Letter illustrate the potential of DWS to study dynamics of systems with multiple scattering. DWS extends QELS to multiple scattering media and is particularly useful for the study of systems with different time scales. All times are probed in backscattering, while the very early times can be probed by transmission. However, to exploit DWS fully, l^* and γ must be measured independently. In addition, an understanding of their dependence on particle size, concentration, and structure factor should be developed. We conclude by noting that our emphasis here has been on the utility of DWS for light scattering. However, the technique should be much more general and be applicable with photons, neutrons, phonons—whenever the diffusion approximation is valid for wave propagation in a disordered medium.

We thank Michael Stephen and Georg Maret for very stimulating discussions and important preprints.

[1]B. J. Berne and R. Pecora, *Dynamic Light Scattering: With Applications to Chemistry, Biology and Physics* (Wiley, New York, 1976).

[2]G. Maret and P. E. Wolf, Z. Phys. B **65**, 409 (1987).

[3]M. J. Stephen, Phys. Rev. B **37**, 1 (1988).

[4]G. H. Watson, Jr., P. A. Fleury, and S. L. McCall, Phys. Rev. Lett. **58**, 945 (1987).

[5]P. W. Anderson, Philos. Mag. B **52**, 505 (1985).

[6]A. A. Golubentsev, Zh. Eksp. Teor. Fiz. **86**, 47 (1984) [Sov. Phys. JETP **59**, 26 (1984)].

[7]P. E. Wolf and G. Maret, Phys. Rev. Lett. **55**, 2696 (1985).

[8]M. P. van Albada and A. Lagendijk, Phys. Rev. Lett. **55**, 2692 (1985); M. P. van Albada, M. B. van der Mark, and A. Lagendijk, Phys. Rev. Lett. **58**, 361 (1987).

[9]P. E. Wolf, E. Akkermans, R. Maynard, and G. Maret, J. Phys. (Paris) **49**, 63 (1988).

[10]E. Akkermans, P. E. Wolf, R. Maynard, and G. Maret, J. Phys. (Paris) **49**, 77 (1988).

[11]D. J. Pine, D. A. Weitz, and P. M. Chaikin, to be published.

[12]A. Ishimaru, *Wave Propagation and Scattering in Random Media* (Academic, New York, 1978).

[13]A. Ishimaru, J. Opt. Soc. Am. **68**, 1045 (1978).

[14]H. M. Lindsay and P. M. Chaikin, J. Chem. Phys. **76**, 3774 (1983), and J. Phys. (Paris), Colloq. **46**, C3-269 (1985).